

See discussions, stats, and author profiles for this publication at: <https://www.researchgate.net/publication/23470740>

Effect of Probe Density and Hybridization Temperature on the Response of an Electrochemical Hairpin-DNA Sensor

ARTICLE *in* ANALYTICAL CHEMISTRY · DECEMBER 2008

Impact Factor: 5.64 · DOI: 10.1021/ac801567d · Source: PubMed

CITATIONS

55

READS

43

4 AUTHORS, INCLUDING:



Hui Peng

East China Normal University

88 PUBLICATIONS 2,179 CITATIONS

SEE PROFILE



Jadranka Travas-Sejdic

University of Auckland

199 PUBLICATIONS 3,478 CITATIONS

SEE PROFILE

Effect of Probe Density and Hybridization Temperature on the Response of an Electrochemical Hairpin-DNA Sensor

Tanja H. M. Kjällman,[†] Hui Peng,[†] Christian Soeller,[†] and Jadranka Travas-Sejdic^{*,†,‡}

Polymer Electronic Research Centre, The University of Auckland, Private Bag 92019, Auckland, New Zealand, and The MacDiarmid Institute for Advanced Materials and Nanotechnology, Wellington, New Zealand

Detection of specific sequences of target DNA is of high importance in many fields, especially in medicinal diagnostics. This study focuses on the response of an electrochemical, label-free DNA sensor at two different hybridization temperatures (37 and 44 °C). The stem-loop structured probes and the blocking polyethylene glycol molecules were self-assembled on the electrode through S–Au bonding, to form a mixed monolayer employed as the sensing platform. Impedance spectroscopy was used for investigation of the electron transfer processes at a modified gold electrode before and after hybridization with the target DNA. The sensor showed sensitive and selective detection of the target DNA at the lower temperature, whereas the higher temperature affected the dynamics of the hairpin significantly, reflected in an increased sensitivity of the sensor.

Gene-sensors show great promise as tools for various applications, such as clinical diagnosis, reliable forensic analysis, environmental monitoring, and biological research. The demand for DNA sensors able to detect single-base mismatches, which are the most common genetic defects that need to be discriminated for medical diagnostic purposes, has become increasingly important.¹ The development of label free, direct, and fast sensors can be essential in meeting that demand. Many of the available strategies for gene detection involve fluorescent,² radioactive, or chemoluminescent markers, which make use of hazardous compounds and are often time-consuming.

Electrochemical impedance can provide the means for detecting the hybridization event with the speed and sensitivity that is needed for the development of an inexpensive, simple, and portable DNA sensor.³ Typically, an electrochemical DNA sensor consists of a solid electrode and a surface-immobilized probe which upon hybridization with its complementary strand, the target, generates an electrochemically detectable signal. In

general, either the single-stranded (ss) probe or the formed double-stranded (ds) DNA is tagged with a redox label that provides the actual signal.³

Tyagi et al. were the first to employ molecular beacons in a solution assay for the detection of DNA hybridization.⁴ Since then molecular beacons have been adapted to surface-immobilized systems which rely on optical as well as electrochemical means of detection.^{5,6} Molecular beacons are single stranded nucleic acid probes, which in the absence of their target strands form hairpin-like secondary structures. The actual probe sequence is situated in the loop part of the strand, and the stem is formed by base-pairing the two complementary arm sequences at either side of the loop. A fluorescent molecule is attached to one end of the probe, whereas a quencher is attached to the other end and in the non-hybridized state the molecular beacon is in a “dark” state. The naturally adopted hairpin structure undergoes a thermodynamically driven conformational change upon hybridization with its complementary strand, forming a double-stranded DNA helix and forcing the fluorescent marker away from the quencher, resulting in a “bright” state.^{4,7} Particularly for solution assays molecular beacons show great ability to distinguish even single-base mismatches from the complementary target sequence⁴ and are therefore suitable probes for sequence-specific detection of their targets. The hairpin secondary structure can also be utilized as a probe without the fluorescent label and the quencher, and thus, the probe used here is referred to as a hairpin probe (HPP) instead of a molecular beacon.

Gold surfaces have been used as a substrate for surface immobilization of ssDNA probes and various anchorage molecules in a range of different DNA detection protocols.^{6,8–11} Gold surfaces offer convenient attachment of thiol-modified molecules to its surface¹² and can also act as the working electrode in electrochemical detection methods. Various thioalkanes and thioalco-

* To whom correspondence should be addressed. Fax: +64 9 373 7499. E-mail: j.travas-sejdic@auckland.ac.nz.

[†] The University of Auckland.

[‡] The MacDiarmid Institute for Advanced Materials and Nanotechnology.

(1) Strohsahl, C. M.; Du, H.; Miller, B. L.; Krauss, T. D. *Talanta* **2005**, *67*, 479–485.

(2) Du, H.; Disney, M. D.; Miller, B. L.; Krauss, T. D. *J. Am. Chem. Soc.* **2003**, *125*, 4012–4013.

(3) Zhang, J.; Song, S.; Zhang, L.; Wang, L.; Wu, H.; Pan, D.; Fan, C. *J. Am. Chem. Soc.* **2006**, *128*, 8575–8580.

(4) Tyagi, S.; Kramer, F. R. *Nat. Biotechnol.* **1996**, *14*, 303–308.

(5) Du, H.; Strohsahl, C. M.; Camera, J.; Miller, B. L.; Krauss, T. D. *J. Am. Chem. Soc.* **2005**, *127*, 7932–7940.

(6) Xu, Y.; Yang, L.; Ye, X.; He, P.; Fang, Y. *Electroanalysis* **2006**, *18*, 873–881.

(7) Dubertret, B.; Calame, M.; Libchaber, A. J. *Nat. Biotechnol.* **2001**, *19*, 365–370.

(8) Steel, A. B.; Herne, T. M.; Tarlov, M. *J. Anal. Chem.* **1998**, *70*, 4670–4677.

(9) Radi, A.-E.; Acero Sanchez, J. L.; Baldrich, E.; O'Sullivan, C. K. *J. Am. Chem. Soc.* **2005**, *128*, 117–124.

(10) Pan, S.; Rothberg, L. *Langmuir* **2005**, *21*, 1022–1027.

(11) Lubin, A. A.; Lai, R. Y.; Baker, B. R.; Heeger, A. J.; Plaxco, K. W. *Anal. Chem.* **2006**, *78*, 5671–5677.

(12) Herne, T. M.; Tarlov, M. *J. Am. Chem. Soc.* **1997**, *119*, 8916–8920.

Table 1. Base Sequences of the Probe and Various Target ODNs

| | oligonucleotide sequence (5' to 3') |
|--|---|
| probe, hairpin 1 | SH-ACACGCTCATCAAGCTTT- AACTCATAGTGAGCGTGT- |
| complementary target, c-DNA | -ACGCTCACTATGAGTTAAAG- CTTG- |
| one-point mismatch target, 1 mm-DNA | -ACGCTGACTATGAGTTAAAG- CTTG- |
| non-complementary target, nc-DNA | -TGAATGAACCTCTTTGCCGG- TGAT- |

hols^{10,13,14} have been used for creating a mixed monolayer to control the surface density of the probes, which is a crucial parameter in the design of a sensitive and selective sensor.^{2,5,6,10,13} Polyethylene glycol (PEG) is known for its ability to make surfaces more biocompatible and for its protein resistance capability.^{15–17} Therefore PEG provides an alternative to thioalkanes or thioalcohols as interstitial spacers in mixed SAMs.^{16–19} PEG spacers are used to reduce nonspecific absorption of the DNA probes to the gold and also to control the probe density on the substrate. Since PEG is an uncharged and very flexible molecule¹⁷ able to provide highly inert interfaces,¹⁹ it is unlikely to interact significantly with the DNA.

This study focuses on the investigation of the response of a label-free, electrochemical DNA sensor based on a mixed self-assembled monolayer (SAM) of hairpin probes and PEG molecules, at two different hybridization temperatures. The interfacial processes at the modified electrode–solution interface are observed as changes in impedance, charge transfer resistance, and current. The sensitivity and selectivity of the sensor is evaluated without any amplification of the response signal.

EXPERIMENTAL SECTION

Materials. The DNA oligonucleotide (ODN) sequences (Table 1) were synthesized by Alpha DNA (Quebec, Canada) and the sequences are listed in Table 1. Thiolated mPEG [$\text{H}_3\text{C}-(\text{CH}_2\text{CH}_2\text{O})_6-\text{CH}_2\text{CH}_2\text{SH}$], molecular weight 356.5 g/mol, was purchased from Polypure (Norway). SSC buffer (10 mM NaCl and 1 mM sodium citrate) and PBS buffer (0.01 M) was prepared using milli-Q water (18.2 Ω cm resistivity).

Pretreatment of Electrodes and Mixed Monolayer Preparation. The gold working electrode was treated with piranha solution ($\text{H}_2\text{SO}_4/\text{H}_2\text{O}_2$ 70/30), rinsed with milli-Q water, and cycled 100 times between -1.2 and -1.8 V (vs Ag/AgCl) in standard PBS solution to obtain a clean gold surface.^{20,21} The electrode was then rinsed with milli-Q water and dried in air. Two immobilization strategies were used: (1) saturation of the gold

surface with hairpin structured probes (HPPs), followed by addition of PEG molecules and (2) simultaneous self-assembly of probes and PEG from a mixture containing a predetermined molar ratio of the two components. The self-assembly of probes and/or PEG on the gold surface was done by placing a 30 μL droplet, with a predetermined probe and/or PEG concentration on the electrode surface. For immobilization strategy (1), initially the probe solution, with a concentration of 4.65 μM (Hairpin 1), was kept at the electrode surface for 30 min in room temperature. The electrode was rinsed thoroughly with SSC buffer to remove any unattached HPPs, followed by back-filling with PEG, deposited in the same manner as the probe, but with a PEG concentration of 46.5 μM and a 1 h immobilization time. The electrode was then thoroughly rinsed again with SSC buffer to remove any remaining unattached PEG molecules and kept in the SSC-buffer for 5 min prior to the measurement. A similar deposition procedure was used for immobilization strategy (2) but various molar ratios of PEG/HPP (2:1, 10:1, and 25:1) were used for simultaneous immobilization during 1 h.

Hybridization. Hybridization was carried out by depositing a 30 μL droplet, with a various concentration of target (ranging between 4.65×10^{-15} M and 4.65×10^{-6} M), on the electrode surface and kept at 37 or 44 $^\circ\text{C}$ for 1 h. After hybridization the electrode was thoroughly rinsed with SSC buffer to remove any non-hybridized target ODN and kept in the SSC-buffer for a minimum of 5 min prior to the measurement.

Electrochemical Measurements. Alternating current (AC) cyclic voltammograms and AC impedance spectra were recorded before the monolayer was formed as well as before and after hybridization using a CH Instruments electrochemical workstation, Model 650C (CH Instruments, U.S.A.). All spectra were measured in SSC buffer containing 5.0 mM $\text{K}_4\text{Fe}(\text{CN})_6/\text{K}_3\text{Fe}(\text{CN})_6$ (1:1 molar ratio) as a redox couple at room temperature. A conventional three-electrode cell with a gold (Au) working electrode (1.6 mm in diameter), an Ag/AgCl (3 M KCl) reference electrode and a platinum (Pt) wire counter electrode, were used. The AC impedance measurements were run at an applied bias potential of 230 mV with a 5 mV sinusoidal excitation amplitude. The data were collected for harmonic frequencies from 0.1 Hz to 0.1 MHz at 1 step per decade and analyzed using the ZView software (version 2.80, Scribner Associates Inc., North Carolina). All experiments have been performed 3 times to test the reproducibility of the sensor responses. It was found that the trends in the sensor responses are reproducible but not the absolute values of the responses. The variations in surface cleaning procedures and the exact composition of the assembled monolayer are considered to be a likely cause of the observed variations. Therefore, a representative sensor response for each case is presented.

Melting Profile of the HPP. The melting profile for the HPP was measured in the PBS buffer, since the target ODNs were diluted with PBS and duplex formation subsequently took place in this buffer, using a UV-1700 Pharmaspec spectrometer from Shimadzu. The UV-spectrometer was connected to a temperature controller, and the temperature was raised from 20 to 80 $^\circ\text{C}$ with a ramp rate of 1 $^\circ\text{C}/\text{min}$. The absorbance was measured once

(13) Lao, R.; Song, S.; Wu, H.; Wang, L.; Zhang, Z.; He, L.; Fan, C. *Anal. Chem.* **2005**, *77*, 6475–6480.

(14) Fan, C.; Plaxco, K. W.; Heeger, A. J. *Proc. Natl. Acad. Sci. U.S.A.* **2003**, *100*, 9134–9137.

(15) Harder, P.; Grunze, M.; Dahint, R.; Whitesides, G. M.; Laibinis, P. E. *J. Phys. Chem. B* **1998**, *102*, 426–436.

(16) Israelachvili, J. *Proc. Natl. Acad. Sci. U.S.A.* **1997**, *94*, 8378–8379.

(17) Jeon, S. I.; Lee, J. H.; Andrade, J. D.; De Gennes, P. G. *J. Colloid Interface Sci.* **1990**, *142*, 149–158.

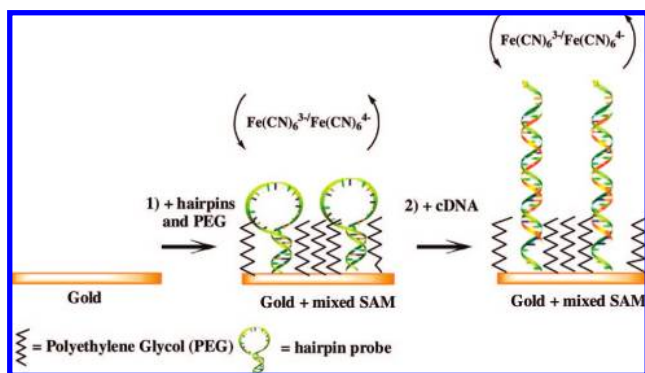
(18) Mrksich, M.; Sigal, G. B.; Whitesides, G. M. *Langmuir* **1995**, *11*, 4383–4385.

(19) Chapman, R. G.; Ostuni, E.; Yan, L.; Whitesides, G. M. *Langmuir* **2000**, *16*, 6927–6936.

(20) Walczak, M. M.; Popenoe, D. D.; Deinhammer, R. S.; Lamp, B. D.; Chung, C.; Porter, M. D. *Langmuir* **1991**, *7*, 2687–2693.

(21) Badia, A.; Arnold, S.; Scheumann, V.; Zizlsperger, M.; Mack, J.; Jung, G.; Knoll, W. *Sens. Actuators, B* **1999**, *B54*, 145–165.

Scheme 1. Schematic Illustration of the Fabrication of the Sensor^a



^a (1) Immobilization of HPP and PEG molecules to the gold electrode and (2) hybridization with complementary ODN.

every degree, at 260 nm. The data was analyzed using the Shimadzu Tm-Analysis software, and the “Two Point Average method” was used to calculate the melting temperature of the HPP. The melting profile of the buffer alone was subtracted from the raw absorbance versus temperature curves of the HPP.

RESULTS AND DISCUSSION

Immobilization of HPP and PEG Molecules onto a Gold Electrode. Scheme 1 shows the stepwise construction of the DNA sensor. Modification of the gold electrode is essential to prepare a suitable platform for DNA hybridization detection. The hybridization efficiency has been found to depend on the secondary structure of the probe, as well as on the distribution of the probe on the substrate.⁵ A hairpin ODN probe, consisting of a stem and loop structure, was chosen as a probe because of its high target recognizing capability.^{4,22} The HPPs and PEG molecules were self-assembled on the electrode by thiol-adsorption to gold,¹² and the electron transfer processes in the self-assembled monolayer (SAM) were investigated primarily through AC impedance but also by AC voltammetry measurements. Probe density is an important parameter in the design of a sensitive and selective sensor;^{3,23} therefore two different immobilization strategies (IS) were used to create the mixed SAM. First, HPPs were allowed to immobilize on the Au surface with the PEGs subsequently backfilled to passivate the surface. Second, simultaneous attachment of both components was performed using a mixture of PEG and HPPs, at a predetermined molar ratio (IS2:1, IS10:1, and IS25:1). A mixed monolayer was chosen as the sensing platform to avoid steric hindrance and probe-probe interactions during the hybridization step. HPPs are more rigid than their single-stranded counterparts, but they are not as rigid as double stranded DNA and are not expected to immobilize in a position completely normal to the Au surface; therefore, nonspecific interactions between the DNA backbone and the Au surface might occur. To minimize these interactions PEG was used to displace any unspecifically attached HPPs and to ensure that they were attached to the surface exclusively through the Au-thiol bond. The PEG molecules used are relatively uncharged and very flexible to minimize any

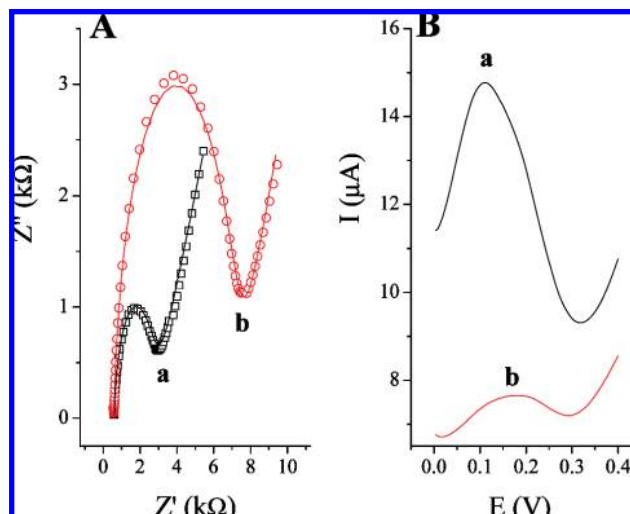


Figure 1. (A) Nyquist plots, $-Z_m$ vs Z_r and (B) Electrochemical AC cyclic voltammograms for a Au electrode in SCC solution containing 5.0 mM $\text{Fe}(\text{CN})_6^{3-}/\text{Fe}(\text{CN})_6^{4-}$: (a) bare Au surface and (b) after immobilization of the hairpin probe (HPP) and PEG molecules.

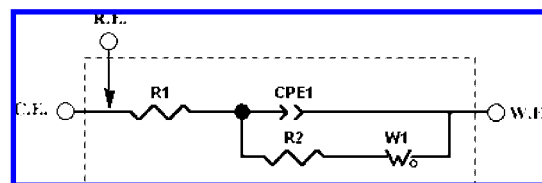


Figure 2. Randles circuit model for a modified Au electrode in a 5.0 mM $\text{Fe}(\text{CN})_6^{3-}/\text{Fe}(\text{CN})_6^{4-}$ electrolyte solution. R_s is the solution resistance, R_{ct} the charge transfer resistance, CPE the constant phase element, and W_0 is the Warburg impedance. WE, RE, and CE are the working-, reference-, and counter-electrode, respectively.

interaction with the HPPs.¹⁹ The approximate height of a PEG molecule with $n = 6$ is 2.5 nm,¹⁵ which is slightly less than the estimated height of the stem in the HPP, 3 nm.²⁴ The complementary target is matched mainly with the loop part of the HPP and therefore the flexible PEGs are not expected to interfere with the hybridization process or the unfolding of the hairpins. A high concentration of probes, which is achieved with immobilization strategy (IS1) resulted in a relatively packed and ordered monolayer even with the short immobilization time used.^{3,10,23} The dense monolayer would force the hairpin probes to an upright position but may also create steric constraints for the hybridization and subsequent unfolding of the hairpins.

In Figure 1A it is shown that the formation of the mixed SAM at the Au electrode surface resulted in a significant increase in the “semicircle” in the Nyquist plot, reflecting an increase in the charge transfer resistance (R_{ct}) at the interface. All the experimental impedance curves were fitted to an equivalent circuit model (Figure 2) that included a solution resistance (R_s) in series with a parallel circuit containing a constant phase element (CPE), the charge transfer resistance (R_{ct}) and Warburg impedance (W_0). The increase in R_{ct} seen after immobilization of HPP and PEG was expected since the molecules in the SAM hindered the electron transfer processes at the electrode surface. The hindered

(22) Tsourkas, A.; Behlke, M. A.; Rose, S. D.; Bao, G. *Nucleic Acids Res.* **2003**, *31*, 1319–1330.

(23) Ricci, F.; Lai, R. Y.; Heeger, A. J.; Plaxco, K. W.; Sumner, J. J. *Langmuir* **2007**, *23*, 6827–6834.

(24) Tinland, B.; Pluen, A.; Sturm, J.; Weill, G. *Macromolecules* **1997**, *30*, 5763–5765.

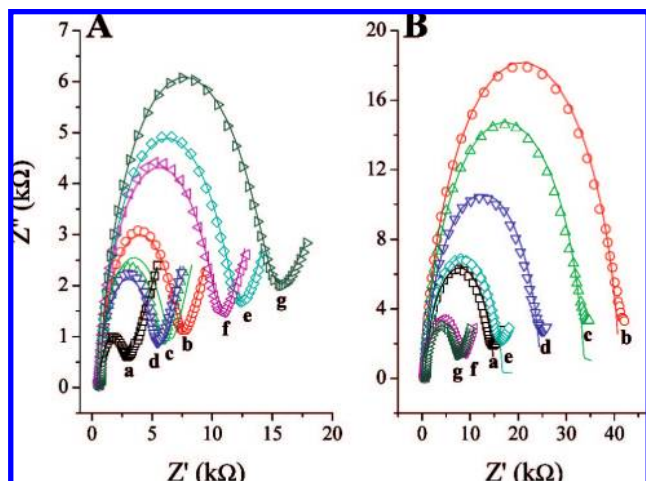


Figure 3. Nyquist plots, $-Z_{im}$ vs Z_{re} for a Au electrode in SCC solution containing 5.0 mM $\text{Fe}(\text{CN})_6^{3-}/\text{Fe}(\text{CN})_6^{4-}$: (a) bare Au surface, (b) after immobilization of the hairpin probe and PEG, after hybridization at (A) 37 °C and (B) 44 °C with (c) 4.66×10^{-15} M, (d) 4.66×10^{-13} M, (e) 4.66×10^{-11} M, (f) 4.66×10^{-9} M, (g) 4.66×10^{-7} M of complementary ODN.

electron transfer was also an indication that a dense monolayer had been formed on the electrode.²⁵ The negative charges on the phosphate backbone of the attached DNA probes repelled the negatively charged redox couple $\text{Fe}(\text{CN})_6^{3-/4-}$, thus further adding to the large R_{ct} . Electron transfer processes through the PEG molecules in the mixed monolayer was ruled out, since a SAM based exclusively on PEG molecules blocked the electron transfer processes at the electrode surface, which resulted in a very high charge transfer resistance of 14.7 MΩ (results not shown). The modified Au electrode was further investigated by AC voltammetry. A considerable decrease in the detected current in the AC voltammogram is seen for the mixed SAM (Figure 1B), supporting the impedance data in Figure 1A.

Hybridization Dynamics and Sensitivity of the DNA Sensor. Hybridization between the hairpin and the target involves both the opening of the stem-loop structure of the probe, as well as the formation of the probe-target duplex, where the probe-target binding is the driving force for the opening of the loop. For the purpose of the later discussion it might be advantageous to the understanding of the hybridization process to describe it as a stepwise event: (1) the target interacts with the probe sequence in the loop and attaches itself to the hairpin, (2) when a sufficient number of bases pairs have been formed the hairpin opens, and (3) the rest of the complementary bases pair up to form the target-probe duplex.²² The Nyquist plots in Figure 3A,B describe the sensor response for various concentrations of complementary target ODN at a hybridization temperature of 37 and 44 °C, respectively. The sensors were prepared by the first immobilization strategy (IS1), resulting in a relatively high probe density layer. The dynamics of the hairpins is dependent on the stability of the hydrogen bonds between the base pairs, which keep the stem together²⁶ and consequently the hybridization temperature plays an important role in the hybridization event; this is reflected

in the distinctively different trends observed in Figure 3A,B. On the basis of the results for the lower hybridization temperature, a general increase in R_{ct} (Figure 3A) can be seen, which reflects the hybridization, but not necessarily the unfolding of the hairpin, and the formation of a stable duplex between the probe and the complementary target ODN. If the hybridization would be considered a stepwise process, as mentioned above, the results suggest that the hybridization can halt at step 1, especially in a sterically crowded environment. However, when a complementary target of a low concentration (pico-molar range) was introduced a decrease in impedance and R_{ct} was observed. A decrease in R_{ct} is an indication of an enhanced electron transfer from the solution to the electrode surface, a behavior expected if the hairpin probes fully unfold upon hybridization. The hairpin probes occupy a larger area on the electrode surface, compared to single stranded probes, and once they unfold completely a bared area of gold will become exposed and thus accessible for the $\text{Fe}(\text{CN})_6^{3-/4-}$, observed as a decrease in the impedance and in the R_{ct} .²⁷ Upon further hybridization the SAM becomes more dense and crowded, and the overall increase in R_{ct} can be explained by an accumulation of negative charges in the monolayer, generated by both the formation of the fully hybridized probe-target duplexes as well as by the partially attached targets to the probe sequence in the hairpin loop. The redox probes in the solution thus experience a stronger repulsion from the SAM after hybridization than before it, increasing the impedance.⁶ An additional concern regarding the effect of steric constraints during hybridization also needs to be considered: even in a case of simultaneous (competitive) immobilization of HPPs and the PEGs a highly heterogeneous distribution of the probes would be expected in the SAM. Some areas may suffer from probe aggregation and thus also from additional steric constraints for the conformational change during hybridization, as observed by Du et al.⁵ The authors concluded that enough target had to be present to open whole “clusters” of molecular beacons before a signal could be detected. A certain extent of bonding between probes could also be possible in locally dense, clustered, areas.⁵ This, along with the rigidity of the hairpins at the lower hybridization temperature could offer an additional explanation to the varying response observed in Figure 3A. To decrease the impedance the hairpins need to fully unfold when the complementary target is introduced. If there are clusters of probes in some areas a sufficient amount of target is needed to unfold all the probes at the same time, as they will be entangled in each other and not very prone to hybridize one by one.⁵ The target will still react with the probe but is unable to open up the hairpin, which results not only in accumulation of negative charges but also of material on the electrode surface, both contributing to the inhibited electron transfer at the electrode surface. On the other hand, once such a cluster of probes simultaneously opens up bare gold is exposed and a decrease in impedance is observed. It is reasonable to believe that at very low target concentrations the sterically favored hairpins will open up first and that the crowded probes will, at least initially, cause the accumulation of target ODN on the surface.

The problem with unfolding of the probes upon hybridization for high probe density sensors can be overcome if additional

(25) Ganesh, V.; Pal, S. K.; Kumar, S.; Lakshminarayanan, V. J. *Colloid Interface Sci.* **2006**, *296*, 195–203.

(26) Bonnet, G.; Tyagi, S.; Libchaber, A.; Kramer, F. R. *Proc. Natl. Acad. Sci. U.S.A.* **1999**, *96*, 6171–6176.

(27) Steichen, M.; Buess-Herman, C. *Electrochem. Commun.* **2005**, *7*, 416–420.

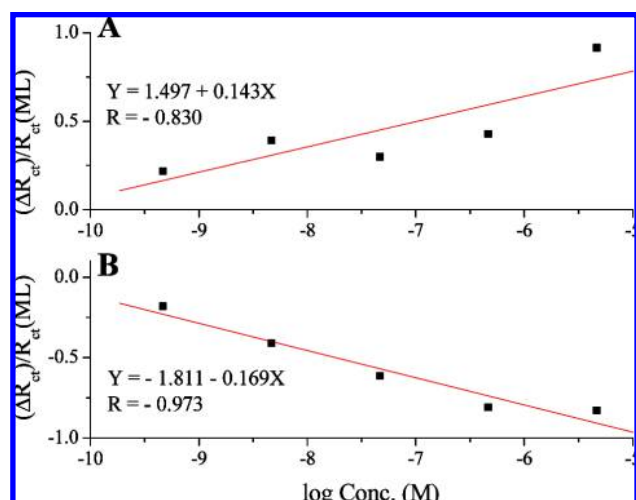


Figure 4. Normalized charge transfer resistance change, $\Delta R_{ct}/R_{ct}(ML)$, taken as the sensor response, before and after hybridization at (A) 37 °C and (B) 44 °C with different concentrations of complementary ODN (4.65×10^{-10} M to 4.65×10^{-6} M) in SCC solution containing 5.0 mM $Fe(CN)_6^{3-}/Fe(CN)_6^{4-}$. The IS1 strategy was used to form the sensing monolayer.

energy (increased hybridization temperature) is introduced during the hybridization event. When a higher hybridization temperature was used an opposite trend could be seen as the impedance decreased continuously upon hybridization with complementary ODN (Figure 3B). It is known that HHPs go through a conformational change upon heating;^{4,22} and to investigate this, a melting profile was measured of the HPP in PBS-buffer (results not shown). A separate profile was measured for the buffer alone, and subtracted from the probe curve to correct for any contribution from the buffer to the sample profile. The melting temperature of a DNA duplex is generally referred to as the midpoint transition where half of the base pairs are broken.²⁸ The two point average method of the software Tm-Analysis was used to calculate the melting temperature, which was found to be 43.6 °C. Cations have a stabilizing effect on DNA duplexes, and the relatively low ionic strength of the PBS buffer used is the likely reason for the low melting temperature of the HPP.²⁸ On the basis of the low melting temperature measured for the HPP (43.6 °C), one can argue that (Figure 3B and Figure 4B) might be due to the opening of the loops by temperature alone and not by target hybridization. This is theoretically possible but ruled out since the electrochemical measurements were conducted at room temperature, not at 44 °C, with a minimum of 5 min in SSC-buffer at room temperature prior to impedance measurements. The HPPs, which might have opened only because of the increased temperature, would have closed again before the impedance was measured. As seen in Figure 5D,H there is no sensor response at very low target concentrations, which provide further evidence that the sensor response is indeed due to duplex formation. At 44 °C the HPPs existed in a transition state, with destabilized stems,^{4,26} making it easier for the target DNA to break the bonds between the base pairs and hybridize efficiently, that is, unfold the hairpin, with the complementary target. Anne and Demaille have shown that even rigid double stranded DNA helices can move in an elastic bending

motion (at 37 °C)²⁹ when attached to a surface. Thus, a destabilization of the stem at the higher hybridization temperature could be expected to enhance the flexibility of the probe within the monolayer, and the target would find the actual probe sequence in the loop part of the probe more easily. The improved flexibility of the probe would thus facilitate the base-pairing with the complementary ODN during the hybridization process. The progressive decrease in the normalized charge transfer resistance, $\Delta R_{ct}/R_{ct}(ML)$, within the applied concentration range of target ODN, also suggested that saturation of the probes had not been reached within this concentration range. ΔR_{ct} represents the difference in charge transfer resistance before and after hybridization with target ODN, and $R_{ct}(ML)$ is the charge transfer resistance for the mixed monolayer before addition of any target ODN.

The sensitivity of this electrochemical sensor can be determined from the dependence of the change in the charge transfer resistance upon hybridization of the hairpin probe on the concentrations of complementary target ODN. Sensitivity is mainly determined by the slope of the linear relationship of response versus concentration.⁶ For the probe hybridized at 37 °C the sensor response is approximately linear with the logarithm of the target concentration with a slope of 0.143 [$\Delta R_{ct}/R_{ct}(ML)$]/[log concentration, (M)] (Figure 4A) whereas a higher sensitivity with a slope of -0.169 [$\Delta R_{ct}/R_{ct}(ML)$]/[log concentration, (M)] (Figure 4B), is found when hybridizing at 44 °C. The sensor response is approximately linear with the logarithm of target concentration in the pico- to micromolar range. The results show that the detection limit could be several orders of magnitude smaller under fully optimized conditions as a reliable response was observed at 50 pM target concentration (taken from the experimental data). The detection limit for a similar type of hairpin sensor, where amplification of the sensor response was achieved by intercalation of an cationic dye into the dsDNA, was found to be 50 pM,⁶ whereas 10 pM concentrations have been detected in a DNA sensing protocol where single stranded probes have been attached on top a mixed SAM, composed of 2-mercaptoethanol and 11-mercaptopundecanoic acid.¹⁰ The sensor investigated here exhibit similar sensitivity, even with an unamplified response.

To gain further insight into the mechanism of the hybridization for the hairpin sensor and to improve the sensitivity of the sensor, various molar ratios of PEG/HPPs were used to create the mixed SAM. The molar ratios used were 2:1, 10:1, and 25:1, and the prepared sensors (IS2:1, IS10:1, IS25:1) were hybridized with a range of complementary target concentrations, from 4.65×10^{-15} M to 4.65×10^{-6} M at both 37 and 44 °C. Figure 5 summarizes the hybridization response from the IS1 sensor at both 37 °C (A) and 44 °C (E) and from the IS2:1, IS10:1, IS25:1 sensors at 37 °C (B, C, D) and at 44 °C (F, G, H). Visualized in Figure 5A–D is the $\Delta R_{ct}/R_{ct}(ML)$ response trend when the probe density was gradually decreased but the hybridization temperature was kept at 37 °C. The dynamic range for the sensor response was defined as the concentration range where the linear fit gives $|R| > 0.900$. In Figure 5A,B,F the $|R|$ value was below 0.900 in the whole concentrations range, and thus, the response of these sensors were not fitted. The response trends can, however, still be

(28) Owczarzy, R.; You, Y.; Moreira, B. G.; Manthey, J. A.; Huang, L.; Behlke, M. A.; Walder, J. A. *Biochemistry* 2004, 43, 3537–3554.

(29) Anne, A.; Demaille, C. *J. Am. Chem. Soc.* 2006, 128, 542–557.

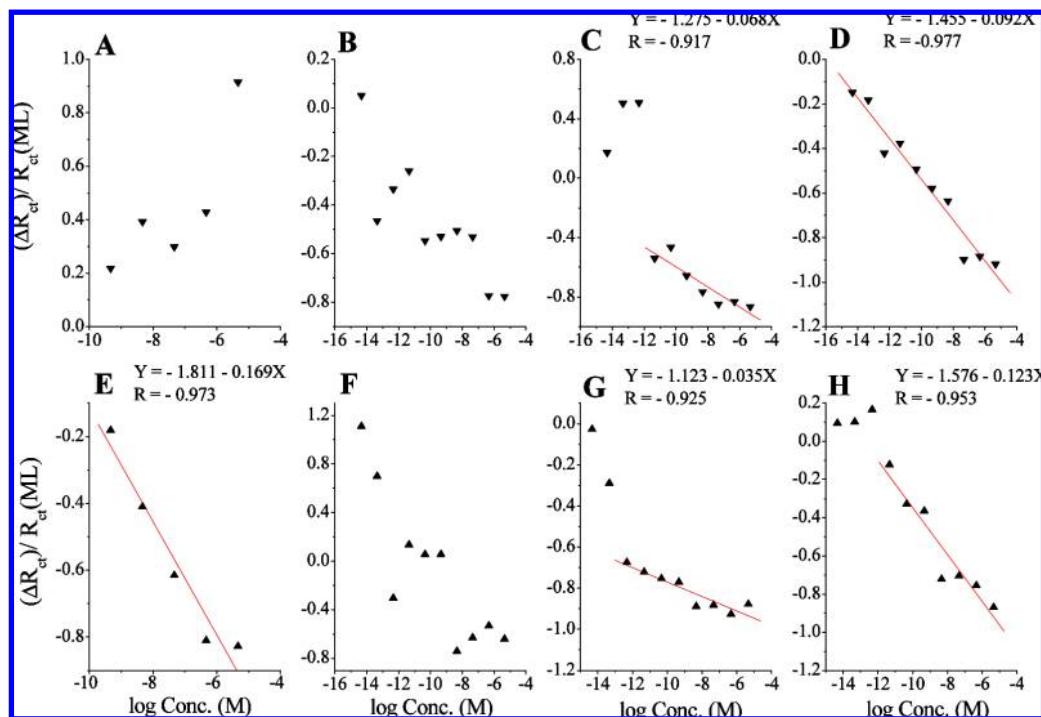


Figure 5. Comparison of $\Delta R_{ct}/R_{ct}$ (ML), taken as the sensor response before and after hybridization with different concentrations of complementary ODN (4.65×10^{-15} M to 4.65×10^{-6} M) in SCC solution containing 5.0 mM $\text{Fe}(\text{CN})_6^{3-}/\text{Fe}(\text{CN})_6^{4-}$. The sensing monolayer was immobilized using either the IS1 strategy (A and E) or IS2:1, IS10:1, and IS25:1 (B, C, D, F, G, and H) with predetermined ratios of PEG/HPP molecules. In Figure 5A–D hybridizations were carried out at 37 °C whereas 44 °C was used in Figure 5E–H.

Table 2. Summary of the Experimentally Determined Detection Limits for the Various Sensors^a

| sensor-immobilization strategy used | detection limit - [pM] | sensitivity-slope of linear response [normalized $\Delta R_{ct}/\log(\text{M})$] | hybridization temperature [°C] |
|-------------------------------------|------------------------|---|--------------------------------|
| IS1 | | | 37 |
| IS2:1 | 0.47 | | 37 |
| IS10:1 | 0.0047 | -0.068 | 37 |
| IS25:1 | 470 | -0.092 | 37 |
| IS1 | | -0.169 | 44 |
| IS2:1 | 0.047 | | 44 |
| IS10:1 | 0.47 | -0.035 | 44 |
| IS25:1 | | -0.123 | 44 |

^a The detection limit was extracted from the experimental data, and defined as the lowest concentration, within the dynamic range of the sensor ($R > 0.900$), where a response could be observed. The sensitivity was determined as the slope of the linear relationship range of response vs concentration.

observed. A progressive shift and stabilization in the response trend of the sensor seemed to be occurring under the investigated conditions (Figure 5A–C), indicating that there still was not enough space for the hairpins to fully open during the hybridization when low concentrations of targets were used, seen as an increase in charge transfer resistance. At higher concentrations of target the impedance starts to decrease, indicating that the probes are able to unfold, resembling the response for lower probe densities at 37 °C (Figure 5C,D) and for most probe densities at 44 °C (Figure 5E,G,H). Table 2 summarizes the experimentally determined detection limits for the various sensors and their sensitivity to complementary target, determined as the slope of the linear relationship range of the response versus the log(concentration). The most reliable and sensitive response was observed

with the IS25:1 sensor at 37 °C (Figure 5D), and the sensor responded to target concentrations as low as 4.66×10^{-15} . Generally a good sensor response was achieved at low probe density for hybridizations performed at 37 °C or high probe density for high hybridization performed at 44 °C, for target concentrations between 4.66×10^{-13} and 4.66×10^{-6} M, (Figures 5C,D,E respectively). The response was linear with $|R|$ values of 0.917 and 0.977 for Figures 5C and 5D, respectively, which is an indication of an efficient and reliable sensor. In Figure 5E a good response is visible for tested target concentrations between 4.66×10^{-10} and 4.66×10^{-6} M with the $|R|$ value of 0.973. When the hybridization temperature was 44 °C the response showed good linearity at target concentrations higher than 4.66×10^{-12} M and an inconsistency in the response at probe densities below 4.66×10^{-12} M (Figure 5G,H). The higher probe density sensor, IS2:1 (hybridization at 44 °C, Figure 5F) showed a behavior similar to the IS2:1 at 37 °C (Figure 5B), indicating that these immobilization strategies do not produce a reliable sensor response.

Selectivity of the DNA sensor. The selectivity of the hairpin probes is generally attributed to the conformation of the stem-loop structure,^{2,4–6,30} and this correlation was also observed for the sensors reported here. The selectivity of a sensor was investigated by measuring the response of the sensor after hybridization with 4.66×10^{-6} M single-base mismatched and 4.66×10^{-6} M non-complementary target ODN at the two different hybridization temperatures. The Nyquist plots in Figure 6A–C show the sensor response for a single-base mismatch target ODN when hybridized at 37 °C. For the high probe density at low hybridization temperature we observed excellent selectivity (Fig-

(30) Fang, X.; Liu, X.; Schuster, S.; Tan, W. *J. Am. Chem. Soc.* **1999**, *121*, 2921–2922.

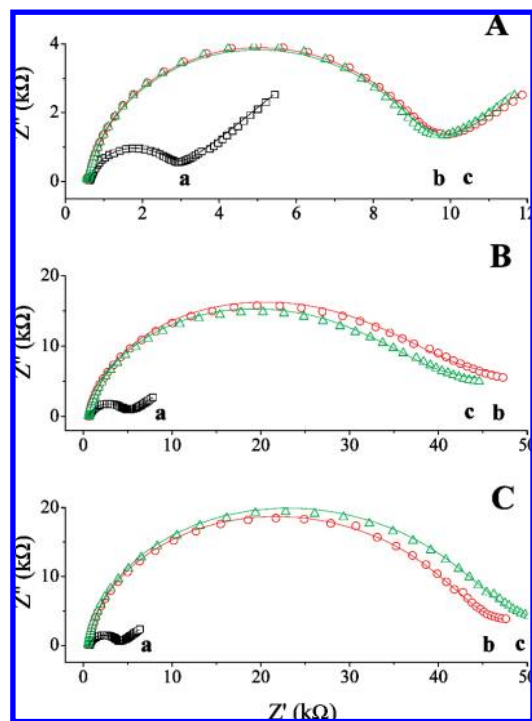


Figure 6. Nyquist plots, $-Z_{im}$ vs Z_{re} and for a Au electrode in SCC solution containing 5.0 mM $\text{Fe}(\text{CN})_6^{3-}/\text{Fe}(\text{CN})_6^{4-}$: (a) bare Au surface, (b) after immobilization of probe and PEG: (A) IS1, (B) IS10:1, (C) IS25:1 and (c) after hybridization at 37 °C with 4.66×10^{-6} M of one-point mismatch ODN.

ure 6A) with no obvious change in the sensor response when the sensor was incubated in a solution of a single-base mismatch target or non-complementary ODN even if their concentration was in the μM range. This indicates a very high selectivity for the target sequence because of the intact conformation of the hairpins in the sterically crowded environment at high probe densities. The response to a non-complementary target almost identically resembled the one-point mismatch response (results not shown), demonstrating that this sensor exhibits an excellent selectivity toward its target sequence.

When the probe density was decreased the selectivity of the sensor, at low hybridization temperature, also started to decrease. At the molar PEG/probe ratio 10:1 (Figure 6B) the sensor responded to the single-base mismatch, but the response was

significantly smaller than for the fully complementary target. The selectivity was not significantly compromised even by the lowest probe density, IS25:1 (Figure 6C), indicating that the stem-loop structure was intact during the hybridization. However, the high selectivity for one-base mismatch targets was lost when hybridization was carried out at 44 °C (results not shown). This is not surprising since the selectivity of the hairpins is known to stem from their secondary structure, which is compromised when the hybridization temperature is close to the melting temperature of the HPP, and thus, selectivity is lost.

CONCLUSIONS

A high-quality DNA sensor can discriminate between its target and mismatched sequences in a reliable and sensitive manner. To realize such a sensor a range of parameters had to be considered and optimized based on the fundamental behavior of the sensing layer. We have presented an electrochemical, label-free sensor based on a mixed self-assembled monolayer (SAM) of polyethylene glycol (PEG) and hairpin structured probes immobilized on a gold electrode. Depending on the hybridization temperature the sensor showed completely opposite trends with regard to the change in charge transfer resistance at the electrode interface. We propose that this difference is due to conformational changes in the transition state of the hairpin at the elevated hybridization temperature. The transition state (partially melted state) allows the hairpin a higher structural flexibility, which facilitates the base-pairing with the complementary ODN and thus assists with the unfolding of the probe.

The best prepared sensor showed sensitivity down to 4.7 fM target ODN and was capable of detecting single-base mismatched ODN. The solid-state approach to DNA sensors is advantageous for practical applications and can provide the basis for miniaturization and manufacturing purposes. Further work to evaluate the sensor reusability is currently underway.

ACKNOWLEDGMENT

The authors thank the Marsden Fund of the Royal Society of New Zealand and the MacDiarmid Institute for Advanced Materials and Nanotechnology for financial support.

Received for review July 25, 2008. Accepted October 19, 2008.

AC801567D